

## Introduction

The northern hemisphere climate of the 20th century has undergone major fluctuations, e.g. an ongoing warming in the arctic region with a decrease in ice-extent. The problem of correctly modelling the ice melt is closely linked to the influence of cirrus clouds on the radiative balance. Through the Norwegian project MACE-SIZ (MARine Climate and Ecosystems in the Seasonal Ice Zone) we study the sensitivity of arctic heat flux and radiative forcing related to various compositions of cirrus clouds and the state of the sea ice-ocean system.



Figure 1: September sea-ice extent predicted from five climate models (ACIA report, 2004): a) Period 2010-2030, b) Period 2070-2090. The seasonal ice zone (SIZ) is defined as the area between the summer minimum and winter maximum extent of the polar ice pack.

## Database

Trough the MACESIZ project we have generated a comprehensive database with size and wavelength dependent extinction cross sections, single scattering albedo, and asymmetry parameters for several ice crystal shapes. The new parameters have been applied in radiative transfer calculations.

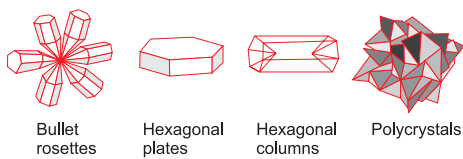


Figure 2: Example of ice crystal shapes.

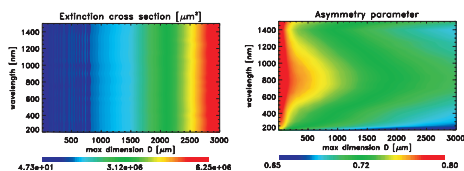


Figure 3: Extinction cross sections and asymmetry parameters for hexagonal plates in the wavelength region 200–1500 nm. Crystal dimensions are from 5 to 3000 μm.

## References:

ACIA. Issued by the Fourth Arctic Council Ministerial Meeting, Reykjavik, 2004  
 Baran, A. J. (2003), *Appl. Opt.*, 42, 2811-2818  
 Ivanova, D., Mitchell, D.L., Arnott, W.P., and Poellot, M. (2001). *Atm. Res.*, 59-60, 89-113  
 Stamnes, K., Tsay, S.-C., Wiscombe, W., and Jayaweera, K. (1988). *Appl. Opt.*, 27, 2502-2509

## Size distribution of ice crystals

In the work we have used ice crystal size distributions from Ivanova (2001) for mid latitude cirrus. The SD is parameterised as bimodal, with both the small and large particle modes being expressed as gamma distributions:

$$N(D) = N_0 D^\nu \exp(-\lambda D)$$

$N_0$ ,  $\nu$ , and  $\lambda$  are calculated for small and large mode.  $N(D)$  is a function of temperature and IWC.

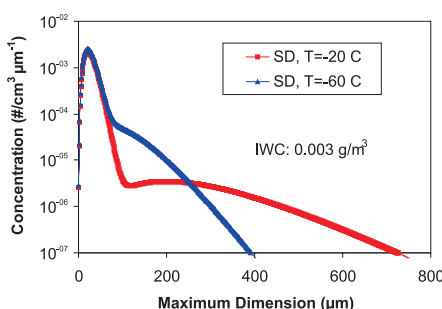


Figure 4: Size distributions of hexagonal columns calculated at -20°C (red line) and -60°C (blue line).

## Representation of cirrus clouds

The cirrus clouds are represented in the radiative transfer model by the extinction coefficients, single scattering albedo, and asymmetry parameters. They are calculated in the following way (for various wavelengths):

$$\bar{C}_{ext}(\lambda) = \int_D n(D) C_{ext}(\lambda, D) dD \quad \text{Extinction cross section}$$

$$\bar{C}_{scat}(\lambda) = \int_D n(D) C_{scat}(\lambda, D) dD \quad \text{Scattering cross section}$$

$$\bar{a}(\lambda) = \frac{\bar{C}_{scat}(\lambda)}{\bar{C}_{ext}(\lambda)} \quad \text{Single scattering albedo}$$

$$\bar{g}(\lambda) = \frac{1}{\bar{C}_{scat}(\lambda)} \int_D n(D) C_{scat}(\lambda, D) g(\lambda, D) dD \quad \text{Asymmetry parameter}$$

$$\text{where } n(D) = N(D)/N_{tot}$$

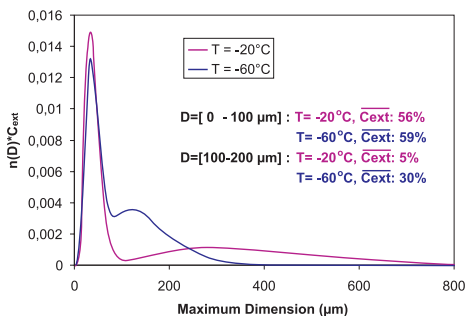


Figure 5: Extinction cross sections for hexagonal columns weighted with the ice crystal size distribution at two different temperatures. At -20°C ice crystals with dimension 100 - 200 μm account for 5% of the cloud optical depth. At -60°C the concentration of ice crystals in the size range 100 - 200 μm increases significantly and they will account for about 30% of the cloud optical depth.

## Radiative transfer calculations

The flux simulations are based on a radiative transfer model (Stamnes et al., 1988) with a subarctic winter profile. In the solar wavelength region the cirrus clouds are composed of various ice crystals (see Figure 2). For flux calculations in the infrared region (4 - 60 μm) it is assumed that the cirrus solely are composed of ice cylinders with dimension 5 to 3500 μm (Baran, 2005).

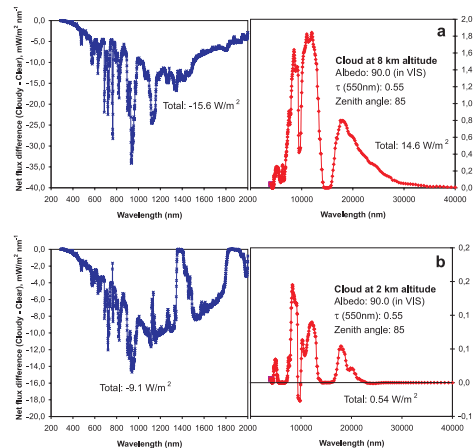


Figure 6: Difference in net downward flux at the top of the atmosphere (TOA) for cloudy vs. clear conditions. The upper and lower panels represent simulations where thin cirrus of hexagonal columns ( $\tau=0.55$ ) are located at altitudes of 8 km and 2 km, respectively. The net cooling effect is most pronounced for the lowest cloud. Also, the cooling effect is strongest for low solar zenith angles (not shown).

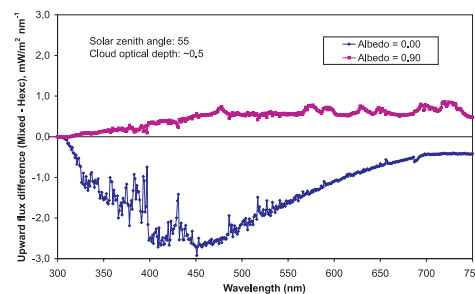


Figure 7: Upward TOA flux differences for cirrus ( $\tau \sim 0.5$ ) with two compositions: a) hexagonal columns and, b) a mixture of hexagonal columns and bullet rosettes (for  $D > 100 \mu\text{m}$ ). Pink and blue line represents different surface albedo.

The blue line in Figure 7 illustrates upward flux differences in the UV/VIS region at zero surface albedo. It shows that cirrus composed of hexagonal columns give higher upward TOA flux than clouds consisting bullet rosettes. When the surface albedo increases to 0.9 a large fraction of the solar radiation will be reflected from the ground. The bullet rosettes, which have the highest asymmetry parameter, will most efficiently scatter the reflected solar radiation back to space.